Cytokine receptor clustering in sensory neurons with an engineered cytokine fusion protein triggers unique pain resolution pathways

Judith Prado[a], Remco H. S. Westerink[b], Jelena Popov-Celeketic[c], Cristine Steen-Louws[a], Aridaman Pandit[a], Sabine Versteeg[a], Wouter van de Worp[a], Deon H. A. J. Kanters[a], Kris A. Reedquist[a], Leo Koenderman[a], C. Erik Hack[a], and Niels Eijkelkamp[a,1]

[a]Center for Translational Immunology, University Medical Center Utrecht, Utrecht University, 3584 EA Utrecht, The Netherlands; [b]Neurotoxicology Research Group, Institute for Risk Assessment Sciences, Faculty of Veterinary Medicine, Utrecht University, 3584 CM Utrecht, The Netherlands; and [c]Department of Rheumatology and Clinical Immunology, University Medical Center Utrecht, Utrecht University, 3584 EA Utrecht, The Netherlands

Edited by David Julius, University of California, San Francisco, CA, and approved February 3, 2021 (received for review May 19, 2020)

New therapeutic approaches to resolve persistent pain are highly needed. We tested the hypothesis that manipulation of cytokine receptors on sensory neurons by clustering regulatory cytokine receptor pairs with a fusion protein of interleukin (IL)-4 and IL-10 (IL4–10 FP) would redirect signaling pathways to optimally boost pain-resolution pathways. We demonstrate that a population of mouse sensory neurons express both receptors for the regulatory cytokines IL-4 and IL-10. This population increases during persistent inflammatory pain. Triggering these receptors with IL4–10 FP has unheralded biological effects, because it resolves inflammatory pain in both male and female mice. Knockdown of both IL4 and IL10 receptors in sensory neurons in vivo ablated the IL4–10 FP-mediated inhibition of inflammatory pain. Knockdown of either one of the receptors prevented the analgesic gain-of-function of IL4–10 FP. In vitro, IL4–10 FP inhibited inflammatory mediator-induced neuronal sensitization more effectively than the combination of cytokines, confirming its superior activity. The IL4–10 FP, contrary to the combination of IL-4 and IL-10, promoted clustering of IL-4 and IL-10 receptors in sensory neurons, leading to unique signaling, that is exemplified by activation of shifts in the cellular kinome and transcriptome. Interrogation of the potentially involved signal pathways led us to identify JAK1 as a key downstream signaling element that mediates the superior analgesic effects of IL4–10 FP. Thus, IL4–10 FP constitutes an immune-biologic that clusters regulatory cytokine receptors in sensory neurons to transduce unique signaling pathways required for full resolution of persistent inflammatory pain.

antiinflammatory cytokines | fusion protein | receptor clustering | inflammatory pain

Chronic pain is a disabling condition and a major clinical problem affecting the quality of life of over 20% of the adult population (1, 2). However, treatments to provide relief from chronic pain are often ineffective or are discontinued due to severe side effects (3). Spontaneous pain, hyperalgesia, and allodynia are common symptoms experienced in chronic pain and are thought to depend on sensitization of the sensory nervous system (4–6). Although chronic pain may at first sight appear to be a neurological problem, evidence indicates that the immune system plays an important role. Cytokines are key players in the regulation of immune responses both in physiological and pathological states. However, cytokines are also key regulators of pain. While proinflammatory cytokines induce pain (7, 8), increasing evidence shows that regulatory cytokines play a role in triggering endogenous pain-resolution pathways. In animal models, spinal interleukin (IL)-10 neutralization with antibodies or by genetic ablation prevents the resolution of inflammatory pain and chemotherapy-induced peripheral neuropathy (9, 10). Moreover, enhanced spinal production of IL-4 and IL-10 in young rodents is linked to reduced development of neuropathic pain after spinal cord injury (11). Importantly, IL-10 levels in cerebrospinal fluid of chronic pain patients are inversely correlated to pain symptoms (12). Furthermore, blood levels of regulatory cytokines, including IL-4 and IL-10, are reduced in patients with chronic pain, including complex regional pain syndrome, chronic widespread pain, and nondiabetic polyneuropathy (12–15).

Regulatory cytokines, such as IL-4 and IL-10, act at different levels in the sensory system. First, they reduce glial activation in several murine models of chronic pain (5, 16, 17) and consequently inhibit the production of glial-derived inflammatory cytokines (18–20). More recent evidence suggests that sensory neurons also respond to regulatory cytokines directly. Subsets of mouse sensory neurons express mRNA for both IL-4 and IL-10 receptors (21). Functionally, IL-10 promotes neurite outgrowth and synapse formation in cultured cortical neurons after injury (22). Importantly, IL-10 relieves neuropathic pain after intrathecal or intracerebral injection in rodents (23–27) and reverses chemotherapy-induced spontaneous firing and hyperexcitability of dorsal root ganglia (DRG) neurons (10, 28). Furthermore,

Significance

Interactions between the immune system and nervous system regulate chronic pain. Cytokines are well-known immune-regulatory molecules that have activities beyond regulation of the immune system, including regulation of pain pathways. We identified that fusion of regulatory cytokines interleukin (IL)-4 and IL-10 into the fusion protein IL4–10 FP provides unexpected properties to inhibit pain by clustering the respective receptor chains of both cytokines in sensory neurons. IL4–10 FP promotes unique signaling pathways and gene-expression profiles that resolve chronic inflammatory pain. Thus IL4–10 FP is an immune biologic that effectively inhibits pain by activating pain-resolution pathways in sensory neurons through clustering of cytokine receptors. This unique effect discriminates IL4–10 FP from a combination therapy with individual regulatory cytokines.

Author contributions: J.P., R.H.S.W., C.E.H., and N.E. designed research; J.P., J.P.-C., C.S.-L., S.V., W.v.d.W., and D.H.A.J.K. performed research; J.P.-C., C.S.-L., K.A.R., and L.K. contributed new reagents/analytic tools; J.P. and A.P. analyzed data; R.H.S.W., C.E.H., and N.E. provided funding; N.E. supervised the work; and J.P. and N.E. wrote the paper.

Competing interest statement: J.P., J.P.-C., C.S.-L., C.E.H., and N.E. have financial interest in Synerkine Pharma BV. Data have been used for patent filings.

This article is a PNAS Direct Submission.

[1]To whom correspondence may be addressed. Email: n.eijkelkamp@umcutrecht.nl.

This article contains supporting information online at https://www.pnas.org/lookup/suppl/doi:10.1073/pnas.2009647118/-/DCSupplemental.

Published March 8, 2021.

IL-4–deficient mice have decreased thresholds to touch as a result of increased spinal neuron activity (29). Conversely, herpes simplex virus-mediated overexpression of IL-4 in DRG alleviates neuropathic pain (30). IL-4 inhibits neuronal activity induced by chemotherapy (paclitaxel)-induced neuronal discharges (31) and induces opioid receptor expression in neuronal cells in vitro (32), which could facilitate pain relief by endogenous secreted β-endorphin. Thus, regulatory cytokines are good candidates to provide analgesia in chronic pain. However, the use of stand-alone cytokines as a pain therapeutic has limitations because of their poor bioavailability and documentation that they can work synergistically in combination (19, 33).

To improve the therapeutic potency of wild-type cytokines, we genetically engineered a fusion protein of the two regulatory cytokines, IL-4 and IL-10. This IL4–10 FP has potent analgesic effects; it inhibits chronic pain more effectively than the mere sum of the combination of the two cytokine moieties. Moreover, multiple injections of the IL4–10 FP completely and permanently resolve chronic inflammatory pain in animal models (19, 34, 35).

Cytokines elicit signaling through homo- or heterodimerization of cell surface receptor chains. The signaling by and functional response to each cytokine depends on the identity of the specific receptor chains it binds (36–40). Intriguingly, cytokine receptor signaling can be redirected via engineered fusion of different cytokines in which each cytokine is mutated to only bind one receptor chain, and as such cause nonnatural dimerization of different cytokine receptor pairs. This nonnatural dimerization of cytokine-receptors generates new signaling programs that differ from those generated by wild-type cytokines under physiological conditions (41). We postulate that the unique analgesic gain-of-function of IL4–10 FP is due to heterologous clustering of IL-4R and IL-10R on neurons.

Results

Sensory Neuron IL-4 and IL-10 Receptors Mediate IL4–10-Induced Analgesia. To identify whether sensory neurons respond to the regulatory cytokines IL-4 and IL-10, we first determined expression of the α-chain of IL-10R, IL-10Rα, and IL-4Rα, the shared chain of all IL-4Rs in murine sensory neurons. In culture, both IL-4Rα and IL-10Rα are expressed in $NF200^-$, peripherin-expressing neurons and nonpeptidergic $IB4^+$ neurons (*SI Appendix*, Fig. S1*A*), often by the same cells (*SI Appendix*, Fig. S1*B*). In vivo, mRNA expression of the receptor chains in sensory neurons of nondiseased mice was confirmed using RNAscope. In mice ∼39% ± 16 (mean ± SD, $n = 4$ mice, 3 DRG per mouse) of sensory neurons expressed the IL-4Rα but not IL-10Rα, while ∼2.7% ± 2.4 expressed IL-10Rα and not IL-4Rα. Sensory neurons that expressed both receptor chains constituted ∼22% ± 16 of the total sensory neuron population (Fig. 1*A*). The proportion of sensory neurons expressing IL-4Rα and IL-10Rα was slightly increased between males and female mice (*SI Appendix*, Fig. S2). IL-10Rα and IL-4Rα protein expression in sensory neurons of nondiseased mice was confirmed using immune-fluorescent staining of the DRG. (Fig. 1*C* and *SI Appendix*, Fig. S3). Next, we assessed whether cytokine receptor chain expression and the proportion of IL-4Rα and IL-10Rα coexpressing sensory neurons is regulated during persistent inflammatory pain. At 6 d after the induction of persistent inflammatory pain the proportion of neurons expressing both cytokine chains had increased up to 49% ± 14, while the proportion of neurons not expressing either of the two cytokine receptor chains had dropped to 3.7% ± 2.6 (Fig. 1 *A* and *B*).

We verified whether IL4–10 FP inhibits persistent inflammatory pain, as shown previously (19), in both sexes. Intrathecal injection of IL4–10 FP at day 6 after induction of persistent inflammatory pain inhibited mechanical hypersensitivity in both females and males to the same extent 24 h after injection (*SI Appendix*, Fig. S4). To test the requirement of IL-4Rα expression in sensory neurons for the analgesic activity of IL4–10 FP, we used intrathecal administration of antisense oligodeoxynucleotides (asODN). This mainly targets IL-4Rα mRNA in cells in the lumbar DRG (42). Three daily intrathecal injections of IL-4Rα asODN reduced IL-4Rα mRNA and protein expression in the DRG by ∼70% compared to mice treated with mismatched (mm) asODN (Fig. 1*D*). IL-4R protein expression was not significantly affected in the dorsal horn of the spinal cord after IL-4Rα asODN (*SI Appendix*, Fig. S5). Intrathecal injection of IL4–10 FP (1 μg) at 6 d after the induction of persistent inflammatory pain completely inhibited carrageenan-induced thermal and mechanical hyperalgesia in female mice treated with mmODN (Fig. 1 *E* and *F*), confirming the potent analgesic properties of IL4–10 FP (19). Notably, the fusion protein did not abolish the ability to sense mechanical or thermal stimuli. Knockdown of IL-4Rα during established carrageenan-induced hyperalgesia did not affect the magnitude of mechanical hypersensitivity. However, IL-4Rα knockdown in the DRG markedly reduced the analgesic effect of IL4–10 FP compared to mice treated with mmODN (Fig. 1 *E* and *F*). To identify the role of IL-10Rα expression in the analgesic properties of IL4–10 FP, IL-10Rα was selectively ablated in $Na_v1.8$-expressing neurons ($Na_v1.8$–IL-$10R^{-/-}$) (Fig. 1 *G*–*I*) that mediate inflammatory pain (43). The course of carrageenan-induced persistent inflammatory hyperalgesia was indistinguishable between wild-type (male and female) and $Na_v1.8$–IL-$10R^{-/-}$ animals. Intrathecal injection of IL4–10 FP (1 μg) at day 6 after induction of inflammatory pain attenuated thermal and mechanical hyperalgesia in wild-type animals. In contrast, deletion of IL-10Rα in $Na_v1.8$-nociceptors partially ablated IL4–10 FP-induced inhibition of both mechanical and thermal hyperalgesia (Fig. 1 *H* and *I*), indicating that nociceptor IL-10Rα is required, in part, for the pain-inhibiting effects of IL4–10 FP.

Since both receptors were required for the full pain-inhibiting effect of the IL4–10 FP, we next tested if ablation of both receptors in sensory neurons would completely prevent the analgesic actions of the IL4–10 FP. To that end, IL-4R expression was knocked down in $Na_v1.8$–IL-$10R^{-/-}$ mice with intrathecal IL-4Rα asODN injections. Knockdown of both IL-4Rα and IL-10Rα did not affect the course of persistent inflammatory pain (Fig. 2 *A* and *B*). Importantly, knockdown of both IL-4Rα and IL-10Rα expression in the DRGs completely abolished IL4–10 FP-induced resolution of pain during the 24 h observation period (Fig. 2 *A* and *B*).

Spinal immediate-early gene c-Fos expression is increased in the dorsal horn of the spinal cord of carrageenan-injected animals (44, 45) and can be used as a proxy of spinal neuronal activation (46, 47). At day 7 after intraplantar carrageenan injection the number of c-Fos^+ neurons in the superficial layers of the dorsal horn was significantly increased compared to naive animals (Fig. 2*C*). Intrathecal administration of IL4–10 FP significantly reduced the number of dorsal horn spinal cord c-Fos^+ neurons (Fig. 2*C*). Knockdown of IL-4Rα and IL-10Rα in sensory neurons completely prevented this IL4–10 FP mediated attenuation of c-Fos expression. Overall, these data demonstrate that both IL-4Rα and IL-10Rα in sensory neurons are required for the full IL4–10 FP-induced inhibition of persistent inflammatory pain.

IL4–10 FP Inhibits Neuronal Sensitization. Proinflammatory mediators sensitize sensory neurons to noxious and innocuous stimuli (4, 48). To test whether IL4–10 FP inhibits inflammatory mediator-induced sensitization of capsaicin-induced calcium responses in sensory neurons, cultured neurons from male and female mice were treated with tumor necrosis factor (TNF) (50 ng/mL) with and without IL4–10 FP (100 ng/mL, 3 nM). The majority of transient receptor potential vanilloid 1 (TRPV1)-expressing sensory neurons expressed IL-4Rα and IL-10Rα (*SI Appendix*, Fig. S6). TNF significantly increased the magnitude of

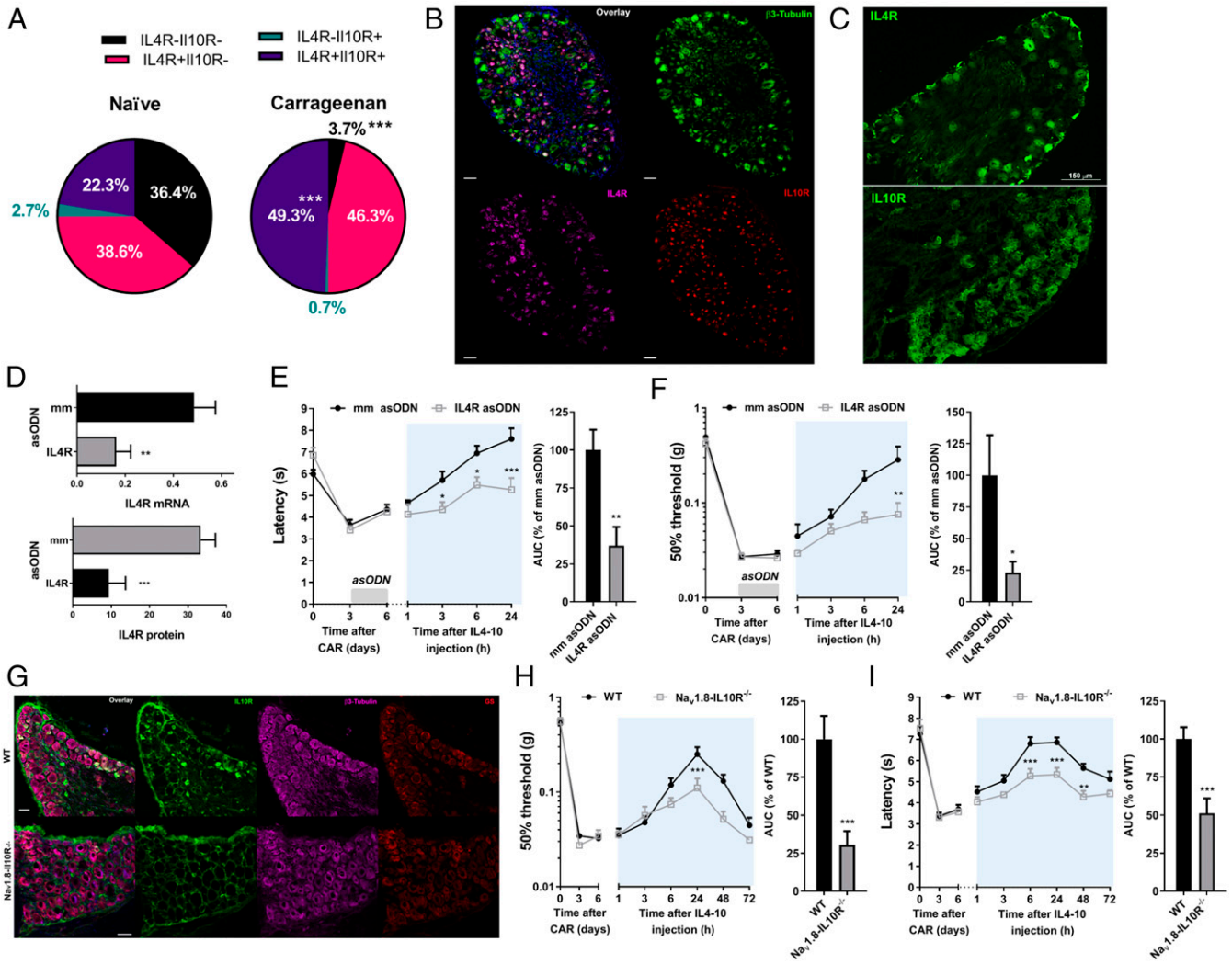

Fig. 1. IL-4 and IL-10 receptors expressed in sensory neurons are required for IL4–10-induced analgesia. (*A*) Pie-chart representation of quantification of DRG neurons double-negative for IL-4Rα and IL-10Rα, IL-4Rα$^+$, IL-10Rα$^+$, or double-positive in nontreated mice (*Left*) or 6 d after intraplantar injection of 20 μL of 2% carrageenan (*Right*). Sample size per condition is three DRGs (L3, L4, L5) per mouse, four mice with two from each sex. (*B*) Representative picture of RNAscope of DRG of mice 6 d after intraplantar injection of 20 μL of 2% carrageenan. (Scale bars, 50 μm.) (*C*) Protein expression of IL-4Rα (*Upper*) and IL-10Rα (*Lower*) in murine DRG. (*D–F*) Persistent inflammatory pain was induced by an intraplantar injection of 20 μL of 2% carrageenan (CAR). At days 3, 4, and 5 after intraplantar injection of carrageenan, female mice received intrathecal injections of mmODN or IL-4R asODN. (*D*) Expression of IL-4R mRNA (*Upper*, n = 13 to 18) and protein (*Lower*, n = 4) in the DRG of IL-4R asODN-treated mice. IL-4Rα mRNA levels were measure with qPCR and corrected for housekeeping genes (actin, GAPDH, and HPRT). Protein expression was determined by quantifying IL-4Rα immunofluorescent staining intensity. Six days after carrageenan administration, female mice received an intrathecal injection of 1 μg IL4–10 FP (n = 5 per group) and (*E*) thermal and (*F*) mechanical sensitivity was followed over time using Hargreaves and Von Frey tests, respectively. *Right* bar graphs represent the analgesic effects of IL4–10 synerkine determined as area under the curve (AUC) between 1 and 24 h after intrathecal injection. (*G*) Immunofluorescence staining of DRG of naïve mice for IL10R expression (green) in DRGs from wild-type (*Upper*) or Na$_V$1.8-IL10R$^{-/-}$ (*Lower*) mice combined with neuronal staining for β3-tubulin (purple) and satellite cell marker glutamine synthetase (GS, red). (Scale bars, 50 μm.) (*H* and *I*) At 6 d after induction of persistent inflammatory pain, WT mice and Na$_V$1.8–IL-10R$^{-/-}$ mice (males [n = 14] and females [n = 13]) received an intrathecal injection of 1 μg IL4–10 FP and (*H*) thermal and (*I*) mechanical sensitivity was followed over time using Hargreaves or Von Frey tests, respectively. *Right* bar graphs represent the analgesic effects of IL4–10 FP determined as AUC for the effect of IL4–10 FP between 1 and 72 h after intrathecal injection. Data are represented as mean ± SEM. Two-way ANOVA, followed by Sidak's multiple comparison test was used in comparisons in *A* and the time-course graphs of *E*, *F*, *H*, and *I*. Significance was tested by unpaired t test (*D*; AUC comparisons in *E*, *F*, *H*, and *I*). *P < 0.05, **P < 0.01, and ***P < 0.001, respectively.

capsaicin-induced calcium influxes compared to untreated cells (Fig. 3*A*). Cotreatment with the IL4–10 FP completely prevented the sensitization of capsaicin-evoked calcium influx by TNF (Fig. 3 *A–C*). Similarly, IL4–10 FP inhibited PGE_2-induced sensitization of capsaicin-induced calcium responses (Fig. 3 *D–F*). These data demonstrate that the IL4–10 FP prevents neuronal sensitization by inflammatory mediators.

To identify whether the inhibitory effects of IL4–10 FP on neuronal sensitization required both cytokine moieties, receptor-blocking antibodies were added (Fig. 3*G*). Blocking either IL-4R or IL-10R slightly reduced the IL4–10 FP-induced inhibition of TNF-induced sensitization of capsaicin-evoked calcium responses. Interestingly, blocking both IL-4R and IL-10R receptors completely abrogated the IL4–10 FP-induced inhibition of neuronal sensitization. Next, we tested whether the effects of the IL4–10 FP on neuronal sensitization are superior to those of the combination of the wild-type cytokines. IL4–10 FP concentration-dependently inhibited TNF-induced sensitization of capsaicin-evoked calcium influx (Fig. 3 *H* and *I*). At a concentration of 3 nM, IL4–10 FP completely reversed TNF-induced sensitization, while the combination

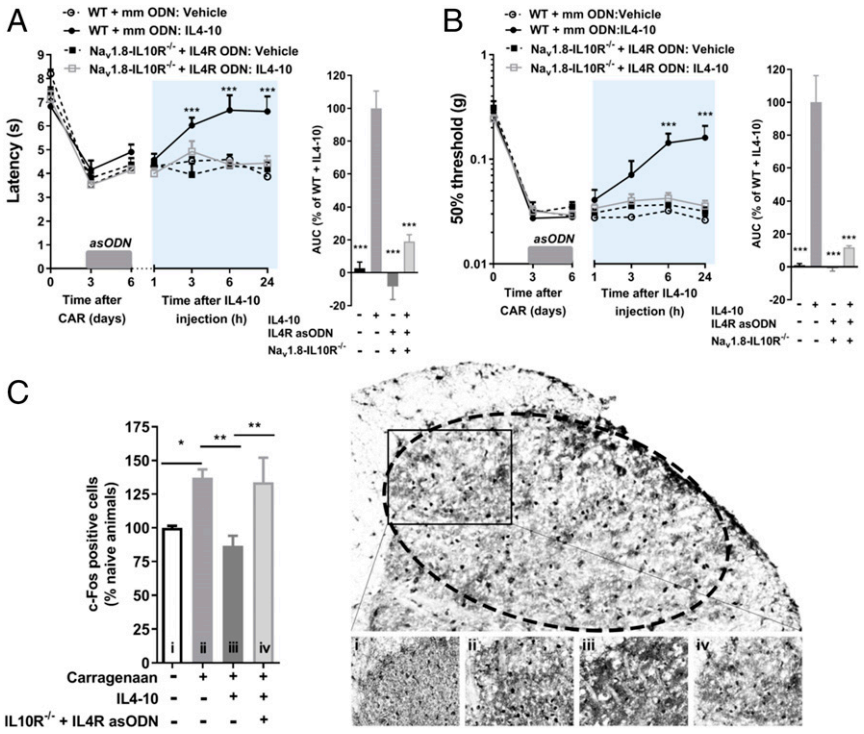

Fig. 2. Knockdown of both IL-4Rα and IL-10Rα in sensory neurons ablates the analgesic effects of IL4–10 FP. Inflammatory pain was induced by an intraplantar injection of 20 μL of 2% carrageenan in wild-type mice or $Na_V1.8$–IL-$10R^{-/-}$. At days 3, 4, and 5 after intraplantar injection, male and female mice received intrathecal injections of mmODN or IL-4R asODN. Six days after intraplantar injection, mice received an intrathecal injection of 1 μg IL4–10 FP and (*A*) thermal and (*B*) mechanical sensitivity was followed over time using Hargreaves or Von Frey tests, respectively ($n = 4$ to 11 per group). *Right* bar graphs represent the analgesic effects of IL4–10 FP determined as AUC between 1 and 24 h after intrathecal injection. (*C*) Quantification of the total number of c-Fos^+ neurons in laminae I to III of the spinal cord 24 h after IL4–10 FP application. (*Right, Upper*) Example c-Fos staining of the superficial dorsal horn of the spinal cord (magnification: 100×). (*Right, Lower*) Representative pictures (magnification: 400×) of c-Fos staining of the dorsal horn of naïve (*i*), carrageenan-injected vehicle-treated WT mice (*ii*), carrageenan-injected IL4–10 FP-treated WT mice (*iii*), and carrageenan-injected IL-4R asODN and IL4–10-treated $Na_V1.8$–IL-$10R^{-/-}$ mice (*iv*) ($n = 4$ to 6 per group). Significance was tested by one-way ANOVA followed by Sidak's multiple comparison test for AUC comparisons in *A*–*C*. Two-way ANOVA followed by Tukey's multiple comparison test was used in time course graphs of *A* and *B*. Data are represented as mean ± SEM, $*P < 0.05$, $**P < 0.01$, and $***P < 0.001$, respectively.

of individual cytokines at the highest dose tested (30 nM) inhibited the TNF-induced sensitization to a maximum of 50% (Fig. 3*I*). These data indicate that fusion of IL-4 and IL-10 into one protein induces a gain-of-potency of IL-4 and IL-10 to reduce neuronal sensitization by inflammatory mediators.

IL4–10 FP Clusters IL-4R and IL-10R in Sensory Neurons. Fusion of IL-4 and IL-10 into one molecule rendered the protein more effective in inhibiting inflammatory pain (19) and neuronal sensitization (Fig. 3 *H* and *I*) than the sum of the individual moieties. We hypothesized that the fusion protein causes heterologous clustering of IL-4R and IL-10R, thereby inducing biased signaling in sensory neurons. Sensory neurons were stimulated with IL4–10 FP or the combination of cytokines for 15 min in vitro followed by a proximity ligation assay (PLA) to assess clustering of IL-4R and IL-10R. This method enabled us to detect clustering of the two receptors within a 51-nm range. IL4–10 (100 ng/mL, 3 nM) treatment clearly clustered IL-4R and IL-10R receptors in sensory neurons, while receptor clustering did not occur after treatment with equimolar concentration of the combination of the cytokines or after vehicle (Fig. 4 and *SI Appendix*, Fig. S7). The IL4–10 FP induced clustering of IL-4R and IL-10R was specific for these receptors because IL-4R and another highly expressed membrane protein, CD200, did not cluster after IL4–10 FP administration (*SI Appendix*, Fig. S8).

IL4–10 FP Induces a Distinct Kinase Activity Profile Compared to the Combination of Cytokines. The ability of IL4–10 FP to cross-link IL-4 and IL-10 receptor chains raised the possibility that this fusion protein drives unique downstream signaling events. To elucidate downstream signaling in sensory neurons in an unbiased manner, we performed PAMgene kinase activity profiling to assess global protein tyrosine kinases (PTK) and serine/threonine kinases (STK) activity after in vivo IL4–10 FP administration in homogenates of lumbar DRG of female mice with persistent inflammatory pain. Kinomic profiles were assessed at 30, 60, and 240 min after intrathecal administration with either the IL4–10 FP, the combination of cytokines or PBS. Analyses of the three different time points indicated that the most prominent changes in kinome profiles between IL4–10 FP and IL-4+IL-10 were present at 60 min after intrathecal injection, with 41 peptides differentially phosphorylated in the PTK chip (*SI Appendix*, Table S1) and 47 peptides in the STK chip (*SI Appendix*, Table S2). At 30 min after treatment with IL4–10 FP, 36 differentially phosphorylated peptides were detected in the PTK (*SI Appendix*, Table S3) and STK (*SI Appendix*, Table S4) chips. At 240 min after treatment with IL4–10 FP, we did not detect differentially phosphorylated peptides. Further analysis, indicated that 38 peptides were also differentially phosphorylated when DRGs from IL4–10 FP-treated mice were compared to DRG homogenates of vehicle-treated mice. Of these, 38 identified substrate peptides, 33 peptides were not significantly phosphorylated by kinases in the DRG homogenates of IL-4+IL-10–treated mice, while 5 peptide substrates were significantly up-regulated by the combination of IL-4 and IL-10, but to a lower extent than in homogenates from IL4–10 FP-treated mice. Overall, these data indicate that IL4–10 FP activates a unique set of PTKs.

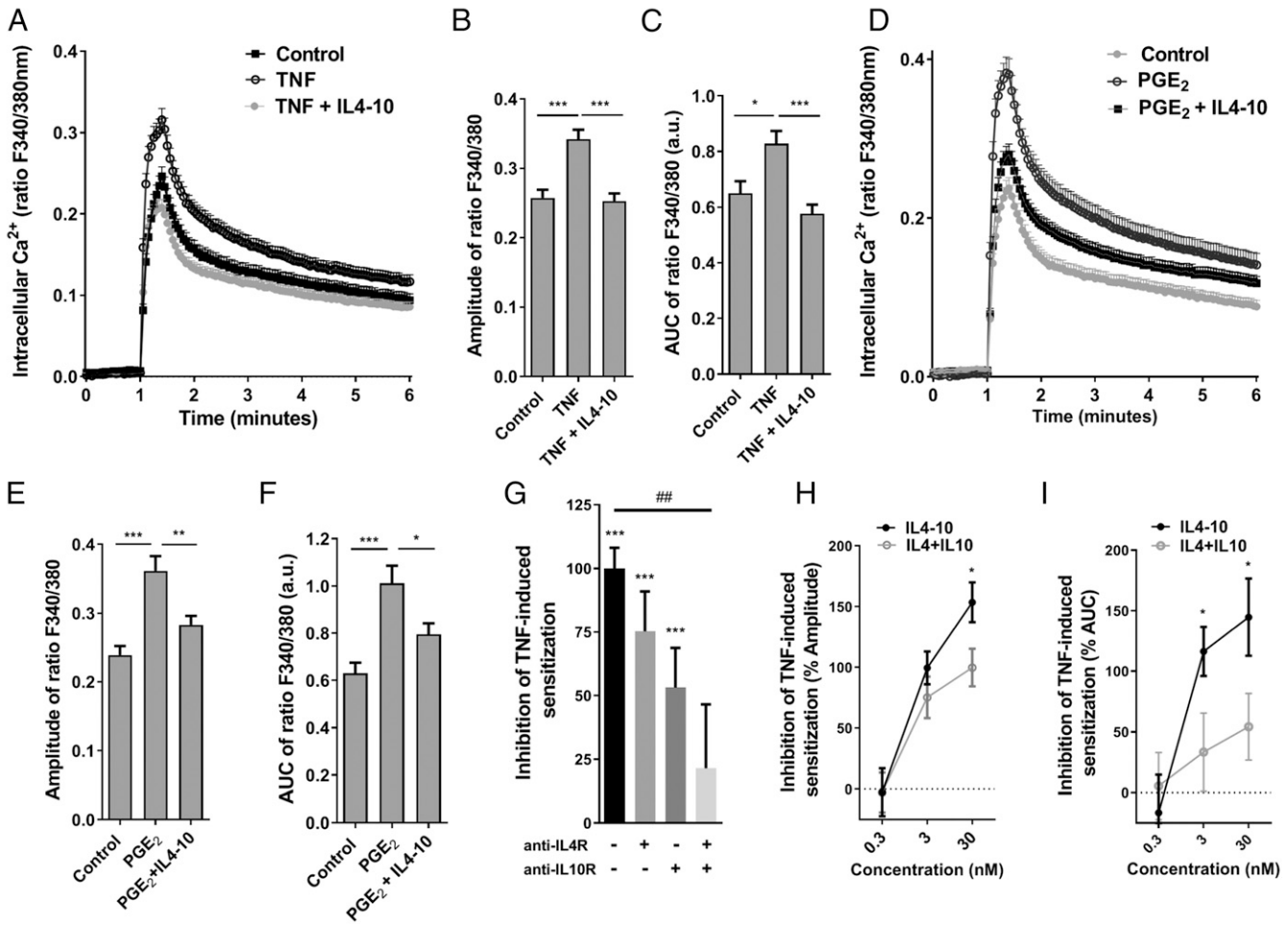

Fig. 3. IL4 –10 FP inhibits inflammatory mediator-induced sensitization of sensory neurons. Fura-2–loaded primary sensory neurons from male and female mice were stimulated with 30 nM capsaicin and Ca^{2+} influx was measured as the ratio of F340/F380 normalized to basal levels. Sensory neurons were stimulated overnight with (*A–C*) TNF (50 ng/mL, $n = 157$ to 244) or (*D–F*) PGE_2 (1 μM, $n = 119$ to 188) in the absence or presence of the IL4–10 FP (100 ng/mL, 3 nM). Total calcium fluxes were quantified by determining the maximal amplitude (*B* and *E*) of capsaicin-evoked Ca^{2+} responses (applied at time point 1 min) and the AUC (*C* and *F*) of capsaicin-evoked Ca^{2+} influx over 5 min. (*G*) Sensory neurons were stimulated overnight with TNF (50 ng/mL) and IL4–10 FP (100 ng/mL) in the presence of receptor-blocking antibodies (2 μg/mL) against the IL-4 receptor (αIL-4R) and the IL-10 receptor (αIL-10R). Inhibition of TNF-sensitization was measured as percentage of AUC of capsaicin-evoked Ca^{2+} response over 5 min. Asterisks represent significant differences compared to the TNF-sensitized neuronal response ($n = 51$ to 164). (*H* and *I*) Sensory neurons were stimulated overnight with TNF (50 ng/mL) in combination with different concentrations (0.3, 3, and 30 nM) of IL4–10 FP or equimolar doses of the combination of both recombinant cytokines. Inhibition of TNF-sensitization was measured as the percentage of the (*H*) amplitude or (*I*) AUC of capsaicin-evoked Ca^{2+} response over 5 min ($n = 107$ to 244). Significance was tested by one-way ANOVA followed by Tukey's multiple comparison test (*B*, *C*, *E*, and *F*). Data are represented as mean ± SEM $^{*}P < 0.05$, $^{**}P < 0.01$, and $^{***}P < 0.001$, respectively ($n = 51$ to 244 from at least 3 different cultures). In *G*, a one-sample *t* test (*) was used to test whether sensitization was still present and a One-way ANOVA followed by Tukey's multiple comparison test to compare differences between groups (##); $^{\#\#}P < 0.01$. In *H* and *I* an unpaired *t* test was used to test for difference between IL4–10 for each concentration.

Evaluation of the differentially phosphorylated serine/threonine kinases peptides by the DRGs of IL4–10 FP versus IL-4+IL-10–treated mice indicated 47 differentially phosphorylated peptides (*SI Appendix*, Table S2). After IL-4 and IL-10 treatment, the majority of peptides were phosphorylated to a lesser extent compared to vehicle-treated mice, indicating inhibition of enzyme activity. In contrast, IL4–10 FP did not affect phosphorylation of these peptides, indicating that IL4–10 FP also activates serine/threonine kinases differentially.

Each of the peptides present in the kinase activity array can be substrates for different kinases, and one kinase or family of kinases can phosphorylate different peptides. To predict the putative upstream kinases activated specifically by the IL4–10 FP, the differential phosphorylation profiles were loaded into PhosphoNET. These analyses predicted that several kinases were differentially activated by IL4–10 FP compared to IL-4+IL-10 at 60 min after injection based on the phosphorylated peptides (Fig. 5*A*). Predicted kinase activation trees activated by either IL4–10 FP (*SI Appendix*, Fig. S9) or IL-4+IL-10 (*SI Appendix*, Fig. S10) were determined based on the differentially phosphorylated peptides when compared to vehicle-treated mice at the different time points.

The rank of top 10 PTK (Fig. 5*B*) and top 10 STK (Fig. 5*C*) differentially regulated by IL4–10 FP or the combination of IL-4+IL-10 were determined according to summation of sensitivity and specificity score. The major differences in kinome activity were observed in PTKs. The PTKs KIT, PDGFRA, FER, MET, and JAK1, and the STKs AKT3, LATS2, NDR2, and CAMK2 were identified as putative downstream signaling kinases differentially activated by IL4–10 FP.

Overall, these data show that IL4–10 FP drives the activation of sets of kinases not activated by the combination of IL-4 and

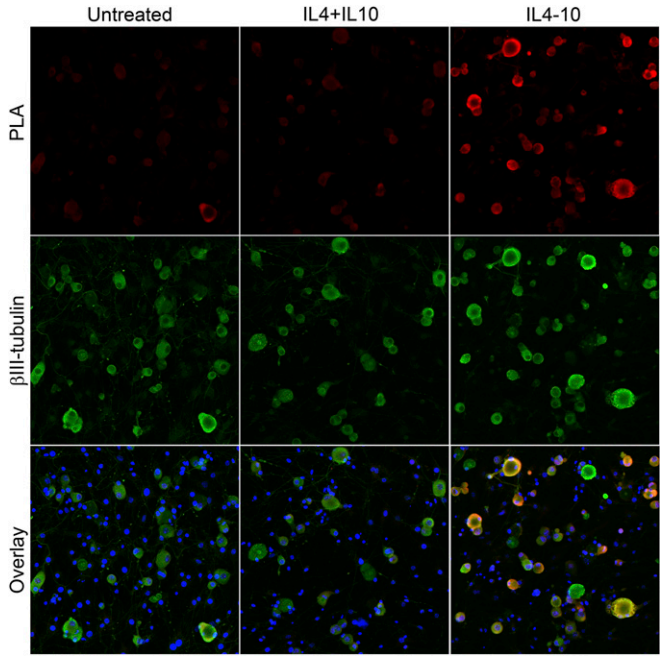

Fig. 4. IL4–10 FP induces heterologous receptor clustering in sensory neurons. Cultured sensory neurons from female mice were treated for 15 min with IL4–10 FP (100 ng/mL; *Right*), the combination of IL-4 and IL-10 (50 ng/mL each; *Center*) or vehicle (*Left*). After fixation PLA for IL-4R and IL-10R was performed (red) and combined with immunofluorescent staining for anti–βIII-tubulin to identify sensory neurons (green). Presence of red fluorescence indicates that IL-4R and IL-10R are at less than 51 nm in proximity to each other. Control staining is shown in *SI Appendix*, Fig. S3.

IL-10 and promotes stronger activation of several kinases also activated by the combination of IL-4 and IL-10.

In Vivo IL4–10 FP Induces a Differential Transcriptome than the Combination of Cytokines. To further explore the potential capacity of the IL4–10 FP to elicit unique downstream effects that differ from that of the combination of IL-4 and IL-10, we performed RNA sequencing (RNA-seq) of DRGs, 6 h after a single intrathecal injection of the IL4–10 FP, the combination of IL-4 and IL-10, or PBS alone in female mice with persistent inflammatory pain. Principal component analysis (PCA) indicated that 75% of the variance in gene expression could be explained by the first two principal components (Fig. 6*A*). The first principal component captured 55% variance of the data and separated the mice injected with IL4–10 FP (shown as green circles in Fig. 6*A*), while the second principal component captured 20% variance of the data and separated vehicle-treated animals (shown as blue circles in Fig. 6*A*), indicating that the fusion protein induced different transcriptome changes. Hierarchical clustering of the top 500 differentially regulated genes shows that, based on their transcriptional profile, the individual animals are grouped together on basis of the three different treatments (Fig. 6*B*). Thus, IL4–10 FP induces a different transcriptional profile compared to mice treated with IL-4 and IL-10 or vehicle.

Treatment of mice with the combination of IL-4 and IL-10 resulted in 4,905 genes differentially expressed (false-discovery rate [FDR]-corrected $P < 0.05$) compared to those injected with PBS (Fig. 6*C*). Kyoto Encyclopedia of Genes and Genomes (KEGG) Pathway analysis indicated that these genes aggregate in pathways affecting Toll-like receptor signaling, oxidative phosphorylation, ribosomal proteins, and lipid metabolism. In the mice injected intrathecally with the IL4–10 FP, 3,995 genes were differentially expressed (FDR-corrected $P < 0.05$) compared to those injected with vehicle (Fig. 6*C*). Pathway analysis of the differentially expressed genes showed that neuronal-related genes, such as axon guidance and calcium signaling, or energy production, such as oxidative phosphorylation were down-regulated in mice treated with IL4–10 FP. Moreover, genes involved in inflammatory pathways, like interferon signaling, antigen processing, and presentation, complement, and IL signaling were affected. Interestingly, when genes induced by IL4–10 FP were compared with the combination of the cytokines, 3,025 genes were differentially expressed (Fig. 6*C*). Analysis of these genes indicated that the expression of 1,650 genes was increased, while 1,375 were down-regulated in the IL4–10 FP group compared to the combination of cytokines. Importantly, 1,675 genes were only regulated by IL4–10 FP but not by the combination of cytokines. From these uniquely regulated genes, the expression of 981 genes was increased by IL4–10 FP, while 694 were down-regulated.

To gain further insight into the potential signaling pathways that could mediate the superior analgesic effects of IL4–10 FP, we identified responsible and upstream kinases of the differential transcriptome induction between IL4–10 FP and IL-4+IL-10 using KEGG pathway analysis. Identified signaling pathways include cytokine and chemokine signaling, NOD-like receptor signaling, and JAK-STAT signaling (Fig. 6*D*). Focal and cell-adhesion molecules and pathways affecting innate and adaptive immune systems, such as Toll-like receptor and T and B cell receptor pathways, indicated potential DRG-infiltrating immune cells (Fig. 6*D*). A more extensive pathway enrichment analysis, including top pathways regulated individually in IL4–10 FP-treated mice or IL-4+IL-10–treated mice is displayed in *SI Appendix*, Fig. S11.

JAK1 Activation Is Required for the Superior Analgesic Effect of IL4–10. Based on the data obtained from PAMgene analysis, we identified KIT, PDGFRA, FER, MET, and JAK1 as the five highest-ranking potential tyrosine kinases linked to the superior effects of IL4–10 FP. This, in combination with identified signaling pathways from the RNA-seq data, led us to test whether JAK1 signaling mediates the superior effects of IL4–10 FP. First, we validated whether IL4–10 FP differentially activates JAK1 in vivo, by assessing phosphorylated (p)JAK1 in sensory neurons 60 min after intrathecal IL4–10 FP injection in female mice with carrageenan-induced persistent inflammatory pain. IL4–10 significantly induced JAK1 phosphorylation in sensory neurons compared to vehicle treatment, while treatment with IL-4 and IL-10 did not (Fig. 7 *A* and *B*).

Next, we investigated if IL4–10 FP also differentially activates JAK1 in sensory neurons in vitro by determining pJAK1 after stimulation of sensory neurons with IL4–10 FP or equimolar concentration of IL-4 and IL-10 for 10, 30, or 60 min. After 10 min, IL4–10 FP significantly increased pJAK1 in sensory neurons compared to vehicle and IL-4+IL-10 (Fig. 7*C*). At 30 min after stimulation, both IL4–10 FP and IL-4+IL-10 increased pJAK1 that had returned to baseline levels at 60 min after stimulation. To investigate whether JAK1 signaling is required for the superior IL4–10 FP analgesic effect, carrageenan-injected female mice were treated with Ruxolitinib (JAK1/2 inhibitor) for 3 consecutive days, starting 1 d before intrathecal administration of IL4–10 FP. Ruxolitinib almost completely prevented the IL4–10 FP-induced inhibition of thermal hyperalgesia (Fig. 7*D*) and shortened the duration of IL4–10 FP-induced inhibition of mechanical hyperalgesia (Fig. 7*E*). Inhibition of JAK1/2 with Ruxolitinib did not affect IL-4+IL-10–induced inhibition of hyperalgesia. To verify whether other kinases that we identified based from PAMgene and RNA-seq data (c-Kit, PDGFR, or c-Met) also contribute to the pain-inhibiting effects of IL4–10 FP we inhibited those kinases using Dasatinib (Kit inhibitor), Masitinib (Kit and PDGFR inhibitor), and JNJ-38877605 (c-Met inhibitor) in female mice. Inhibition of c-Kit or combined inhibition

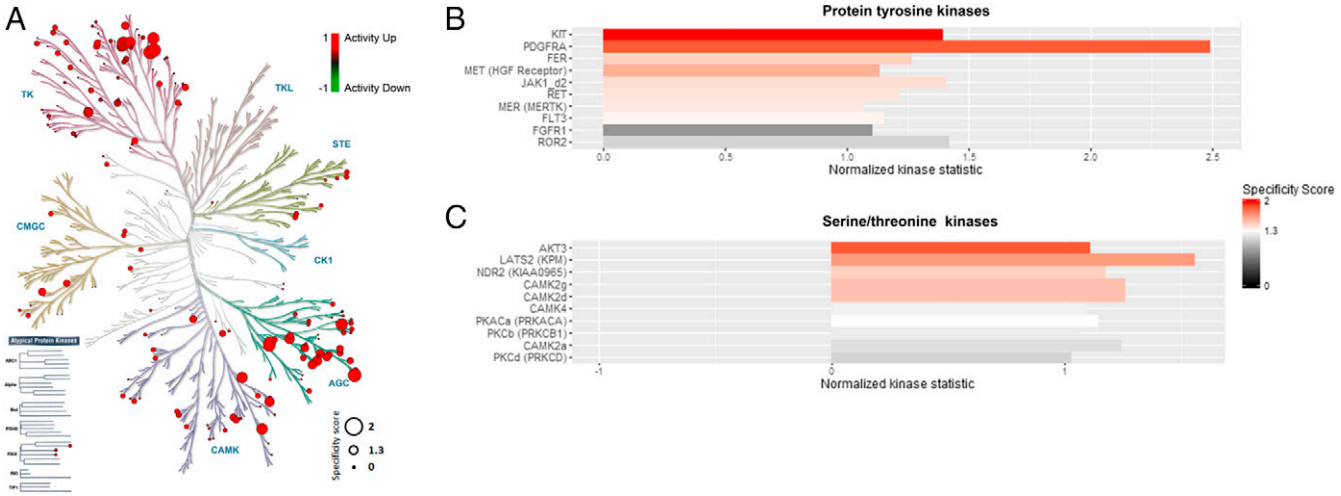

Fig. 5. Kinome activity profiling of the DRG after IL4–10 FP or IL-4+IL-10 administration. Female mice received an intraplantar injection of 20 μL of 2% carrageenan and 6 d later received an intrathecal injection with either vehicle, the combination of IL-4+IL-10 (0.5 μg each), or IL4–10 FP (1 μg). One hour after intrathecal injection, DRGs were isolated and DRG homogenates were subjected to PAMgene analysis. (*A*) Predicted upstream kinases that can be inferred from the peptide substrates differentially phosphorylatedon the PAM chips identified by unpaired *t* test comparison between samples from IL4–10-treated animals compared to IL-4+IL-10–treated animals ($n = 5$ animals per group). Illustration reproduced in courtesy of Cell Signaling Technology, https://www.cellsignal.com/. (*B*) Top 10 predicted protein tyrosine kinases and (*C*) top 10 predicted serine/threonine kinases differentially regulated between samples from IL4–10-treated animals compared to IL-4+IL-10–treated animals.

of c-Kit and PDGFR did not affect IL4–10 FP-induced inhibition of thermal hyperalgesia (Fig. 7*F*). In contrast, inhibition of c-Kit and both c-Kit and PDGFR enhanced the IL4–10 FP-induced reduction in mechanical hyperalgesia by IL4–10 FP (Fig. 7*G*). Pharmacological inhibition of c-Met partially attenuated the pain-inhibiting effects of IL4–10 FP (Fig. 7 *F* and *G*). Intraperitoneal injection of either Dasatinib or Masitinib in mice with persistent inflammatory pain did not affect mechanical thresholds (*SI Appendix*, Fig. S12). Thermal hypersensitivity was slightly but significantly reduced only at 6 h after injection, but this effect was not present at 24 h after injection. Thus, pJAK1 and to some extent c-MET signaling is required for the superior pain-alleviating effect of IL4–10 FP.

Discussion

In the present work, a unique mechanism by which pain-resolution pathways are fully triggered by the clustering of IL-4 and IL-10 receptors with a fusion molecule of two regulatory cytokines, IL4–10 FP. Our work demonstrates that sensory neurons express functional IL-4R and IL-10R, but that triggering of these receptors by the combination of IL-4 and IL-10 is not sufficient to fully inhibit neuronal sensitization and to resolve chronic inflammatory pain in mice (19). Moreover, we demonstrate that fusing IL-4 and IL-10 into a single entity, IL4–10 FP, yields a molecule that causes heterologous clustering of IL-4 and IL-10 receptor chain complexes in sensory neurons in vitro. This clustering triggers unique pathways, not activated by the combination of both wild-type cytokines, that result in complete resolution of chronic inflammatory pain in mice. Knockdown of either IL-4R or IL-10R individually resulted in loss of this unique biological effect of IL4–10 FP (i.e., full resolution of pain), leaving it with analgesic activity comparable to the combination IL-4 and IL-10, whereas ablation of both receptors in the DRG totally abrogated the analgesic activity of IL4–10 FP. Thus, we show that combining two regulatory cytokines into a single entity creates a molecule that induces unique signaling through dimerization of cytokine receptors in sensory neurons which can be exploited to optimally trigger pain resolution pathways and stop persistent inflammatory pain. Notably, IL4–10 FP also inhibited neuropathic pain (19), chemotherapy-induced neuropathy (10), and osteoarthritis pain (49). As such IL4–10 FP constitutes an immunobiologic with unprecedented properties to fully resolve persistent pain.

Proinflammatory cytokines are well known for their ability to induce pain by depolarizing and sensitizing sensory neurons through activating cytokine receptors expressed in these cells (7, 8). The role of regulatory cytokines in regulating sensory neurons is poorly understood. Recently, a few reports have shown that regulatory cytokines directly modulate neuronal responses. Both IL-4 and IL-10 reduce the number of neuronal ectopic discharges induced by chemotherapy treatment (10, 28, 31). Moreover, IL-4 regulates opioid receptor expression in cultured neuronal cells (32), while IL-10 down-regulates voltage-gated sodium channels in DRGs (23) and promotes neurite growth and synapse formation in vitro (22). We show here that IL-10R and IL-4R are expressed by sets of sensory neurons in mice, are subject to regulation during persistent inflammatory pain, and that these receptors are pivotal for the analgesic action of a fusion protein of the regulatory cytokines IL-4 and IL-10, confirming the importance of regulatory cytokine to control in vivo sensory neuron functioning. IL4–10 FP inhibits neuronal sensitization induced through completely different pathways, namely cytokine receptor-mediated or through G protein-coupled receptors. Thus, the fusion protein is likely capable to interfere with sensitization by a variety of inflammatory mediators that act through different receptor pathways.

We show here that IL-4R and IL-10R are expressed by sensory neurons of mice and their expression is subject to regulation by peripheral inflammation. Importantly, the proportion of sensory neurons expressing both cytokine receptors is substantially larger during persistent inflammatory pain than in naive conditions. Thus, a peripheral inflammation renders sensory neurons innervating the inflamed tissue sensitive to the regulation by IL-4 or IL-10. Though the physiological role of this up-regulation remains to be understood, our findings imply that a large proportion of sensory neurons (~50%) may be sensitive to clustering of IL-4R and IL-10R by the IL4–10 FP during inflammatory pain. To what extent these data can be translated to humans remains to be established as mouse and human DRG show differences with respect to cell biology and biochemistry. Analysis of available transcriptomic data (50) indicates that human DRG express IL-4Rα and IL-10Rα (*SI Appendix*, Fig. S13). Future research should reveal

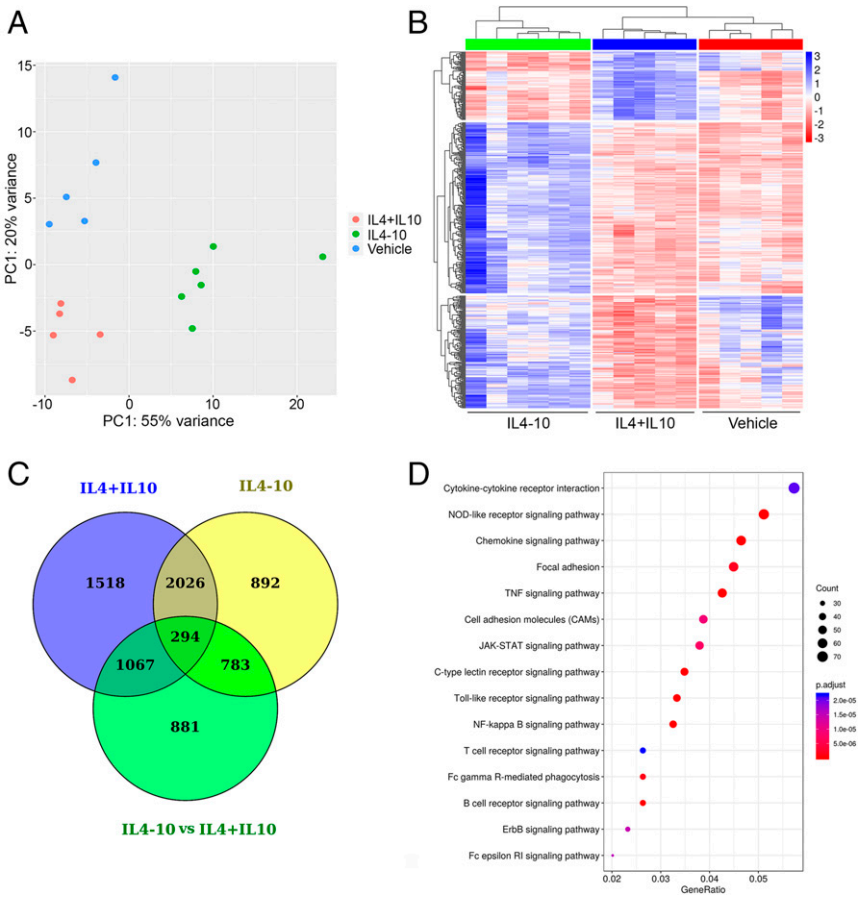

Fig. 6. Transcriptome analysis of the DRG after intrathecal injection of IL4–10. Persistent inflammatory pain was induced by an intraplantar injection of 20 μL of 2% carrageenan. Six days later, female mice received an intrathecal injection of vehicle (control, $n = 5$), IL-4+IL-10 (0.5 μg each, $n = 5$) or IL4–10 FP (1 μg, $n = 6$). Six hours after intrathecal injection, lumbar DRGs (L3–L5) were isolated and subjected to RNA-seq. (*A*) PCA of the differentially expressed genes in all pairwise comparisons of different animal. (*B*) Hierarchical clustering heat map of the expression levels of the top 500 differentially expressed genes (based on adjusted *P* values). (*C*) Venn diagram showing the number of differentially expressed genes in IL4–10 FP or IL-4+IL-10–treated animals compared to vehicle-treated animals. (*D*) Pathway enrichment analysis of the differentially regulated transcript (IL4–10 FP versus IL-4+IL-10) to identifying potential signaling pathways upstream of the differentially regulated genes.

whether the proportion of human neurons expressing both receptors is comparable to their murine counterparts.

Intrathecal administration of asODN mainly targets sensory neurons in the DRG (42, 51, 52). Indeed, we did not observe significant reduction of IL-4Rα in the dorsal horn of the spinal cord upon such administration. Yet, we cannot rule out that IL-4R asODN may have reduced IL-4R in cells other than neurons in the DRG, such as satellite cells or immune cells infiltrating the DRG. Moreover, glial cells express IL-4R and we previously demonstrated that the IL4–10 FP inhibited spinal glial activation in a model of persistent inflammatory pain (19). In vitro, IL4–10 FP also reduced proinflammatory cytokine release by glial cells, but the effect is predominantly caused by the IL-10 moiety of IL4–10 FP.

Although we have previously shown that IL4–10 FP can directly inhibit glial cells (19), we show here that cytokine receptors expressed by sensory neurons are required for full pain resolution. Importantly, IL4–10 FP inhibits sensory neurons in a superior fashion in vitro compared to equimolar concentrations of IL-4 and IL-10. In contrast, the potency of IL4–10 FP to inhibit glia is comparable to that of IL-4+IL-10 combined (19). It remains to be determined whether this difference between regulation of sensory neurons and glia is due to the relative expression of cytokine receptors expressed in the specific cells or the outcome measures assessed in vitro (LPS-induced TNF production versus TNF-induced sensitization of TRPV1 response). Although the expression of IL-4R and IL-10R in sensory neurons is required for the effect of IL4–10 FP, our data do not exclude that a part of the effect of IL4–10 FP is mediated through triggering these receptors on spinal glial cells. IL4–10 FP may also indirectly inhibit glia by reducing the production and secretion of molecules by sensory neurons that modulate microglial activation, such as colony-stimulating factor 1 (CSF-1) or ATP (53–55). Interestingly, RNA-seq analysis revealed that IL4–10 FP downregulates neuregulin-1, a protein secreted by damaged sensory neurons to engage spinal cord microglia (56). The property to inhibit both sensory neurons and glia cells, endows IL4–10 FP with the unique capability to combat chronic pain at multiple levels: That is, functional aberrations in sensory neurons and glial cells, in addition to its effects on the production of proinflammatory cytokines that trigger pain.

We show here that the fusion of IL-4 and IL-10 into a single molecule generates a protein with unique properties. We suggest that the unique properties of IL4–10 FP result from its ability to cluster different regulatory cytokine receptors in sensory neurons. A fusion protein of the growth factor GM-CSF combined with common γ-chain ILs into a single, bifunctional polypeptide also clusters different cognate receptors and causes hyperactivation of downstream JAK-STATs (57–59). Indeed, it is becoming clear that recruiting receptor chains of cytokine receptors together that are naturally not clustered induces novel signaling programs and may

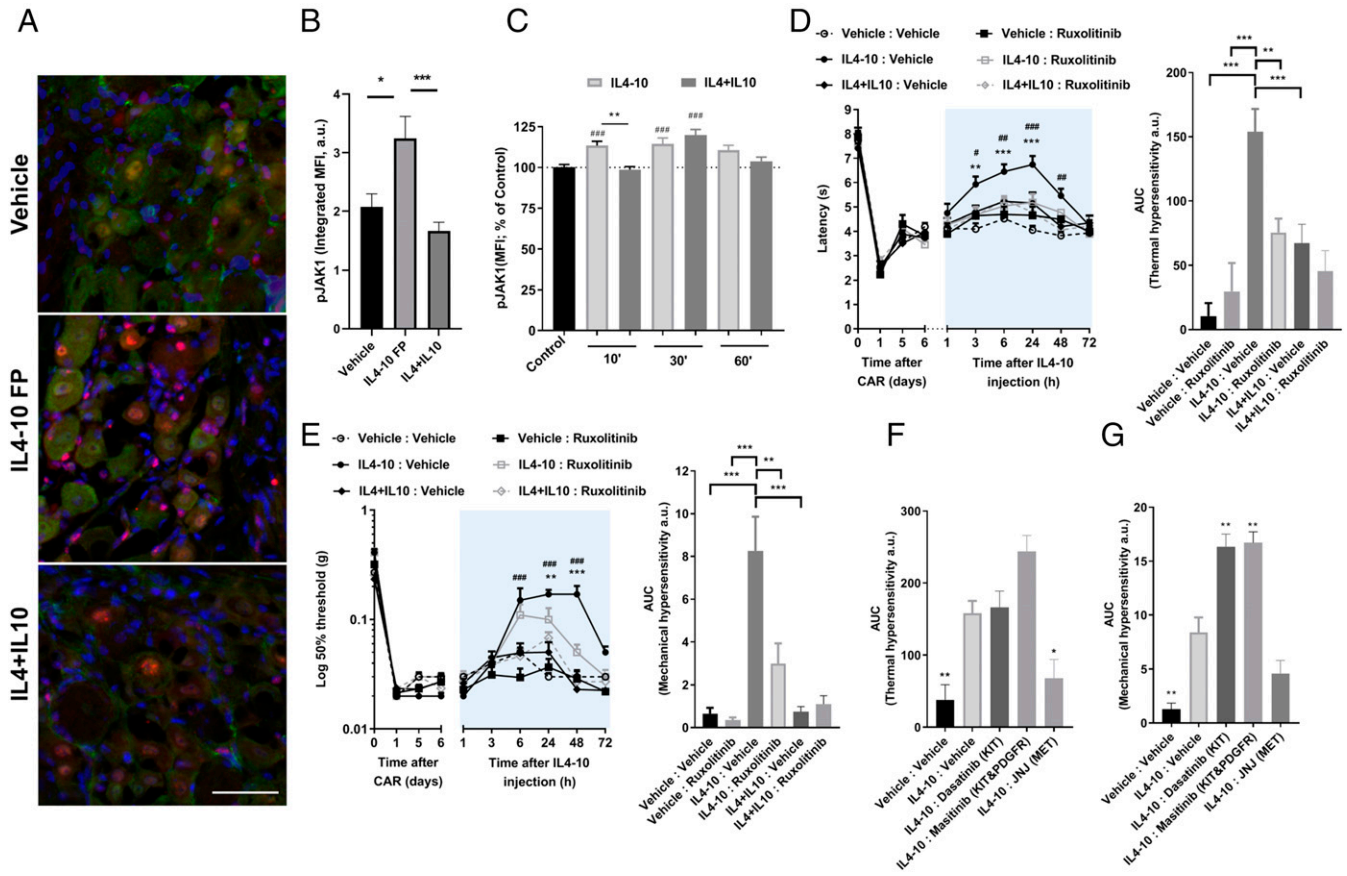

Fig. 7. Role of JAK in the analgesic effect of IL4–10 FP. Female mice with carrageenan-induced persistent inflammatory pain were intrathecally injected at day 6 with vehicle, 1 μg IL4–10 FP or equimolar dose of IL-4+IL-10. One hour after injections, lumbar DRG were collected. (*A*) Representative pictures of pJAK1 staining (red) combined with neuronal marker NeuN (green) and nuclear staining DAPI (blue) in DRG. (Scale bar, 25 μm.) (*B*) Quantification of pJAK1 staining ($n = 6$ DRG obtained from three animals per group). (*C*) Sensory neurons were treated in vitro for 10, 30, or 60 min with IL4–10 FP (100 ng/mL; light gray columns), the combination of IL-4 and IL-10 (50 ng/mL each; dark gray columns) or vehicle (black column). Cells were stained for pJAK1 and fluorescence intensity of individual cells were measured. Data are obtained in four different independent primary neuronal cultures. (*D*–*G*) Persistent inflammatory pain was induced by an intraplantar injection of 20 μL of 2% carrageenan. (*D* and *E*) At days 5, 6, and 7 after intraplantar injection, female mice received Ruxolitinib (JAK1/2 inhibitor; $n = 8$) or vehicle orally ($n = 4$). Six days after intraplantar injection, mice received an intrathecal injection of 1 μg IL4–10 FP ($n = 8$) or PBS as vehicle ($n = 4$) and (*D*) thermal and (*E*) mechanical sensitivity was followed over time using Hargreaves or Von Frey tests, respectively. *Right* bar graphs represent the total analgesic effects of IL4–10 synerkine determined as AUC between 1 and 72 h after intrathecal injection. $^{*}P < 0.05$ IL4–10: Vehicle versus IL4–10: Ruxolitinib-treated mice. $^{\#}P < 0.05$ IL4-–10: Vehicle versus IL-4+IL-10: Vehicle-treated mice. (*F* and *G*) Six days after intraplantar injection of carrageenan mice received an intrathecal injection of 1 μg IL4–10 FP and (*F*) thermal and (*G*) mechanical sensitivity was followed over time using Hargreaves or Von Frey tests, respectively. To inhibit c-Kit or both c-Kit and PDGFR, mice received respectively intraperitoneal injections of Dasatinib ($n = 4$), or Masitinib ($n = 4$) at days 5, 6, and 7 after intraplantar carrageenan injection. To inhibit MET, mice were orally administered with the MET inhibitor JNJ-38877605 ($n = 5$) or vehicle. Bar graphs represent the analgesic effects of IL4–10 FP determined as AUC between 1 and 72 h after intrathecal injection. Significance was tested by one-way ANOVA followed by Tukey's multiple comparison test (*B*, *C*, *F*, and *G* and AUC comparisons panel in *D* and *E*). Two-way ANOVA followed by Sidak's multiple comparison test was used for course of hyperalgesia in *D* and *E*. Data are represented as mean ± SEM; $^{*}P < 0.05$ or $^{\#}P < 0.05$; $^{**}P < 0.01$ or $^{\#\#}P < 0.01$; $^{***}P < 0.001$ or $^{\#\#\#}P < 0.001$.

affects cellular function differentially than the natural signaling programs do (41). Our data further extend this concept; IL4–10 FP clusters of IL-4R and IL-10R in vitro and differentially and uniquely activates several tyrosine and serine/threonine kinases, with JAK1 signaling being hyperactivated in vitro and in vivo. We hypothesize that this biased signaling by IL4–10 FP causes the unique transcriptome changes in the DRG associated with pain resolution.

We identified JAK1 activation as a key signaling event required for the superior effects of IL4–10 FP. Intriguingly, chronic itch is dependent on neuronal IL–4Rα and JAK1 signaling suggesting the IL-4R and JAK1 do play opposing role in itch and pain regulation (60). Both IL-10 and IL-4 induce JAK1 phosphorylation, though extensive JAK1 signaling is mostly linked to downstream signaling of IL-4 (reviewed in ref. 61). Despite a primary role for JAK1 in mediating the analgesic effect of IL4–10 FP, we cannot exclude the contribution of other differentially activated kinases. Kinase activity profiling revealed that IL4–10 FP activates a unique set of kinases, including Kit, PDGFR, and Met kinases. It will be important to unravel how these kinases individually, or in concert, contribute to the resolution of persistent inflammatory pain.

In line with its potency to activate a unique set of kinases, IL4–10 regulates some genes not affected by the combination therapy of IL-4+IL-10, as revealed by RNA-seq analysis. Some of these uniquely down-regulated genes are members of the neurotrophin signaling family, such as the tropomyosin-related kinase receptor (TrK) C and Sortilin, both related to pain modulation (62, 63). Strikingly, the majority of genes up-regulated by the fusion protein are immune related genes. These genes include markers of macrophages, such as CD68 and CD11b, and in

particular also M2 macrophages markers, such as Arginase 1, Cd200r1, IL-4I1, or Ym1. Moreover, the increase in T cell markers, such as CD3, CD28, CD8, FoxP3, ctla4, and Icos suggest possible infiltration of CD8 regulatory T cells in the DRG. Indeed, CD8 T cells have a regulatory role in pain, because they inhibit pain in models of inflammatory, chemotherapy, and nerve injury-induced pain (10, 64, 65). Thus, it is well possible that IL4–10 FP promote the release of factors by sensory neurons that attract immune cells. In agreement herewith, expression of several chemokines—such as CCL-2, -3, -4, -5, -6, -7, -9, and -19, and CXCL-1, -2, -9, -10, or -13—were up-regulated in the DRGs of IL4–10 FP-treated animals. The role of these immune cells in the analgesic effect of IL4–10 FP remains to be determined. Recently, a role for myeloid cells in pain regulation has gained attention (20). The differentiation of macrophages into proinflammatory (M1) or regulatory (M2) phenotypes can induce pro- or antinociceptive effects, respectively. Moreover, depletion of macrophages in the DRG prevents the resolution of transient inflammatory pain, indicating that these macrophages contribute to the resolution of pain (9, 66).

The need for novel therapeutics devoid of undesirable side effects to treat chronic pain is significant. Current analgesics, such as opioids and nonsteroidal antiinflammatory drugs, are notorious because of their limited effectiveness in chronic pain and their severe side-effects. We here report the molecular mechanisms of IL4–10 FP, a fusion protein of regulatory cytokines with potent analgesic effects on inflammatory pain, as well as in models for neuropathic and osteoarthritis pain (10, 19, 49). Importantly, IL4–10 FP is based on endogenous protein sequences and has a unique safety profile, being devoid of typical side effects of current analgesics, such as gastrointestinal bleeding, cardiovascular events, respiratory suppression, and addiction. The unique mechanism of action of IL4–10 FP results from its ability to cluster non-natural receptor dimers of IL-4R and IL-10R. We suggest that heterologous clustering of cytokine receptors by fusion proteins of regulatory cytokines is a strong concept for developing novel therapeutics in chronic pain, and possibly other diseases.

Materials and Methods

All methods are detailed in *SI Appendix* and briefly described here.

Animals. All animal experiments were performed in accordance with international guidelines and with prior approval from the local experimental animal welfare body and the national Central Authority for Scientific Procedures on Animals (CCD, AVD115002015323). Experiments were conducted with 8- to 14-wk-old male and female wild-type C57BL/6 mice (Envigo). To obtain *Nav1.8*^{Cre}*Il10r*^{flox} mice, floxed IL-10R mice (67) were crossed with $Na_v1.8$-Cre mice (68).

Persistent Inflammatory Hyperalgesia and Behavioral Assays. Mice received an intraplantar injection of 20 μL λ-carrageenan (2% [wt/vol]; Sigma–Aldrich) dissolved in saline (NaCl 0.9%) in both hind paws (19). Heat-withdrawal latency times were determined using the Hargreaves test (IITC Life Science) (69). Mechanical thresholds were assessed in both hind paws using the Von Frey test (Stoelting) with the up-and-down method to determine the 50% threshold (70).

For both Hargreaves and Von Frey tests, values of both paws were averaged. Observers who performed these tests were blind to the mouse genotype and treatment.

Drugs and Administration. The IL4–10 FP was produced in HEK293 cells and purified as described previously (19). Intrathecal injections of different compounds (5 μL per mouse) were performed as described previously (71) under light isoflurane/O_2 anesthesia. The IL4–10 FP (1 μg per mouse) or equimolar doses of recombinant human IL-4 and IL-10 (Sigma) were injected intrathecally at day 6 after intraplantar λ-carrageenan injection.

IL-4Rα expression in sensory neurons was knocked down by intrathecal injections of asODN directed against IL-4Rα mRNA (72). This approach has been shown to successfully inhibit the expression of several proteins in DRG neurons (42, 73). Kinase inhibitors were administered for 3 consecutive days starting 1 d before intrathecal administration of IL4–10 or IL-4+IL-10.

Culture of DRG Neurons. DRGs were cultured as described previously (74). Cells were seed on poly-L-lysine (0.01 mg/mL; Sigma) and laminin (0.02 mg/mL; Sigma)-coated glass coverslips in a 5% CO_2 incubator at 37 °C. Cells were used the following 1 to 2 d.

For investigation of JAK1 signaling, DRG neurons cultured for 24 h followed by serum deprivation for 4 h before stimulation with IL4–10 FP (200 ng/mL) or the combination of IL4 and IL10 (100 ng/mL each, respectively) for 10, 30, or 60 min and then fixed in 4% PFA

Calcium Imaging. DRG neurons used for calcium imaging experiments were stimulated overnight with TNF (50 ng/mL, Peprotech) with or without the IL4–10 FP (100 ng/mL; 3 nM), recombinant IL4 and IL10 (50 ng/mL each; 3.3 and 2.9 nm, respectively), and/or receptor blocking antibodies against mouse IL-4R or IL-10R (2 μg/mL; BD Pharmingen).

Changes in the capsaicin-evoked calcium response were measured by loading cells with 5 μM Fura-2-AM (Invitrogen). Recordings were performed as previously described (75), with minor modifications detailed in *SI Appendix*.

Tissue Processing and Immunochemistry. Mice were anesthetized with an injection of pentobarbital (60 mg/kg, intraperitoneal) and transcardially perfused with phosphate-buffered saline (PBS) followed by 4% paraformaldehyde (PFA) in PBS. Lumbar DRGs and spinal cords (lumbar L3–L5 section) were isolated, postfixed in 4% PFA cryoprotected in sucrose, and embedded and frozen in optimal cutting temperature compound. Details of the staining can be found in *SI Appendix*.

RNA Extraction and Quantitative PCR. Lumbar DRGs were homogenized using TRIzol (Invitrogen). Total RNA was extracted using the RNeasy Mini Kit (Qiagen) and 1 μg of total RNA was used to synthesize cDNA. cDNA was synthesized using SuperScript reverse transcriptase (Invitrogen). RNA concentrations were determined using a NanoDrop 2000 (Thermo Scientific).

The real-time PCR using SYBRgreen master mix (Bio-Rad) was performed on an iQ5 Real-Time PCR Detection System (Bio-Rad). Primers used for qPCR are listed in *SI Appendix*, Table S5 (*SI Appendix, Supplementary Materials and Methods*). The mRNA expression levels were normalized for GAPDH, HRPT and actin. Primers details can be found in *SI Appendix*.

RNAscope In Situ Hybridization. RNAscope in situ hybridization multiplex v2 was performed as instructed by Advanced Cell Diagnostics on fresh frozen tissue was cut at 10-μM thickness. Slides were then processed for immunohistochemistry with anti–β3-tubulin antibody (ab18207, Abcam; 1:1,000) or anti-TRPV1 antibody (PA1-29770, Thermofisher; 1:300) overnight at 4 °C.

In Situ PLA. IL-4Rα antibody was labeled to thiol-MINUS-oligo with the dual cross-linker sulfo-SMCC (ThermoFisher). IL-10Rα antibody was labeled with biotin using EZ-Link Sulfo-NHS-LC-Biotin SMCC (ThermoFisher). Primary DRG cultures were treated with IL4–10 FP (100 ng/mL; 3 nM) or the combination of IL-4 and IL-10 (50 ng/mL each; 3.3 and 2.9 nM, respectively) for 15 min and fixed with 4% PFA for 10 min. In situ PLA was performed as described previously (76), with some modifications and detailed in the *SI Appendix*.

Kinase Activity Profiling. Lumbar DRGs were homogenized using M-PER mammalian Extraction buffer (Pierce) supplemented with phosphatase and protease inhibitor mixtures (Pierce). Protein concentration was determined using the Bradford assay (77) (Bio-Rad). Kinase activity profiling was performed using the Tyrosine Kinase PamChip (PTK) Array and the Serine/Threonine Kinase PamChip (STK) Array for Pamstation12 (PamGene International).

RNA-Seq. RNA libraries were prepared with the poly(A) selection method followed by multiplexing and sequencing on the Illumina NextSeq500 platform in a 1 × 75-bp single-read and 350 million reads per lane (Utrecht Sequencing Facility). All samples passed the read quality checks performed using FastQC (78). The sequencing reads from each sample were aligned to the recent reference human genome GRCh38 build 79 assembly from Ensembl (Genome Reference Consortium Mouse Build 38) using the STAR aligner (79, 80).

Statistical Analysis. All data are presented as mean ± SEM as indicated in the figure legends and were analyzed with GraphPad Prism version 8.3.0 using unpaired two-tailed *t* tests, one-way or two-way repeated-measures ANOVA, followed by post hoc analysis. The statistical test used are indicated in each figure legend. A *P* value less than 0.05 was considered statistically

significant, and each significance is indicated with $*P < 0.05$ or $^{\#}P < 0.05$; $**P < 0.01$ or $^{\#\#}P < 0.01$; $***P < 0.001$ or $^{\#\#\#}P < 0.001$.

Data Availability. The data reported in this paper have been deposited in the Gene Expression Omnibus (GEO) database, https://www.ncbi.nlm.nih.gov/geo (accession no. GSE150795) (81).

ACKNOWLEDGMENTS. We thank Werner Müller (University of Manchester, Manchester, UK) for providing us with IL-10Rα^{Loxp} mice; Bea Malvar Fernandez (University Medical Center Utrecht) and Savithri Rangarajan (PamGene International) for PAMgene support; Fiona Wijnolts for calcium imaging support; and the Utrecht Sequencing Facility for providing sequencing service and data. The Utrecht Sequencing Facility is subsidized by the University Medical Center Utrecht, Hubrecht Institute, Utrecht University, and The Netherlands X-omics Initiative (Dutch Research Council Project 184.034.019). This work has received funding from the Life Sciences Seed grant of the University Utrecht. This work is part of the research programme "Open Technology Programme" with Project 16907, which is (partly) financed by the Dutch Research Council.

1. H. Breivik, B. Collett, V. Ventafridda, R. Cohen, D. Gallacher, Survey of chronic pain in Europe: Prevalence, impact on daily life, and treatment. *Eur. J. Pain* **10**, 287–333 (2006).
2. B. Gerdle *et al*., Prevalence of widespread pain and associations with work status: A population study. *BMC Musculoskelet. Disord.* **9**, 102 (2008).
3. D. Borsook, C. M. Aasted, R. Burstein, L. Becerra, Migraine mistakes: Error awareness. *Neuroscientist* **20**, 291–304 (2014).
4. K. Ren, R. Dubner, Interactions between the immune and nervous systems in pain. *Nat. Med.* **16**, 1267–1276 (2010).
5. M. B. Graeber, M. J. Christie, Multiple mechanisms of microglia: A gatekeeper's contribution to pain states. *Exp. Neurol.* **234**, 255–261 (2012).
6. R. R. Ji, A. Chamessian, Y. Q. Zhang, Pain regulation by non-neuronal cells and inflammation. *Science* **354**, 572–577 (2016).
7. N. Ghasemlou, I. M. Chiu, J. P. Julien, C. J. Woolf, CD11b+Ly6G- myeloid cells mediate mechanical inflammatory pain hypersensitivity. *Proc. Natl. Acad. Sci. U.S.A.* **112**, E6808–E6817 (2015).
8. A. C. Ozaktay, J. M. Cavanaugh, I. Asik, J. A. DeLeo, J. N. Weinstein, Dorsal root sensitivity to interleukin-1 beta, interleukin-6 and tumor necrosis factor in rats. *Eur. Spine J.* **11**, 467–475 (2002).
9. H. L. Willemen *et al*., Monocytes/Macrophages control resolution of transient inflammatory pain. *J. Pain* **15**, 496–506 (2014).
10. K. Krukowski *et al*., CD8+ T cells and endogenous IL-10 are required for resolution of chemotherapy-induced neuropathic pain. *J. Neurosci.* **36**, 11074–11083 (2016).
11. R. McKelvey, T. Berta, E. Old, R. R. Ji, M. Fitzgerald, Neuropathic pain is constitutively suppressed in early life by anti-inflammatory neuroimmune regulation. *J. Neurosci.* **35**, 457–466 (2015).
12. M. M. Backonja, C. L. Coe, D. A. Muller, K. Schell, Altered cytokine levels in the blood and cerebrospinal fluid of chronic pain patients. *J. Neuroimmunol.* **195**, 157–163 (2008).
13. N. Uçeyler, T. Eberle, R. Rolke, F. Birklein, C. Sommer, Differential expression patterns of cytokines in complex regional pain syndrome. *Pain* **132**, 195–205 (2007).
14. N. Uçeyler *et al*., Reduced levels of antiinflammatory cytokines in patients with chronic widespread pain. *Arthritis Rheum.* **54**, 2656–2664 (2006).
15. A. G. Vanderwall, E. D. Milligan, Cytokines in pain: Harnessing endogenous anti-inflammatory signaling for improved pain management. *Front. Immunol.* **10**, 3009 (2019).
16. S. Echeverry *et al*., Transforming growth factor-beta1 impairs neuropathic pain through pleiotropic effects. *Mol. Pain* **5**, 16 (2009).
17. E. D. Milligan, K. R. Penzkover, R. G. Soderquist, M. J. Mahoney, Spinal interleukin-10 therapy to treat peripheral neuropathic pain. *Neuromodulation* **15**, 520–526, discussion 526 (2012).
18. J. Mika, M. Zychowska, K. Popiolek-Barczyk, E. Rojewska, B. Przewlocka, Importance of glial activation in neuropathic pain. *Eur. J. Pharmacol.* **716**, 106–119 (2013).
19. N. Eijkelkamp *et al*., IL4-10 fusion protein is a novel drug to treat persistent inflammatory pain. *J. Neurosci.* **36**, 7353–7363 (2016).
20. R. Raoof, H. L. D. M. Willemen, N. Eijkelkamp, Divergent roles of immune cells and their mediators in pain. *Rheumatology (Oxford)* **57**, 429–440 (2018).
21. D. Usoskin *et al*., Unbiased classification of sensory neuron types by large-scale single-cell RNA sequencing. *Nat. Neurosci.* **18**, 145–153 (2015).
22. H. Chen *et al*., IL-10 promotes neurite outgrowth and synapse formation in cultured cortical neurons after the oxygen-glucose deprivation via JAK1/STAT3 pathway. *Sci. Rep.* **6**, 30459 (2016).
23. K. F. Shen *et al*., Interleukin-10 down-regulates voltage gated sodium channels in rat dorsal root ganglion neurons. *Exp. Neurol.* **247**, 466–475 (2013).
24. R. G. Soderquist *et al*., Release of plasmid DNA-encoding IL-10 from PLGA microparticles facilitates long-term reversal of neuropathic pain following a single intrathecal administration. *Pharm. Res.* **27**, 841–854 (2010).
25. A. G. Vanderwall *et al*., Effects of spinal non-viral interleukin-10 gene therapy formulated with d-mannose in neuropathic interleukin-10 deficient mice: Behavioral characterization, mRNA and protein analysis in pain relevant tissues. *Brain Behav. Immun.* **69**, 91–112 (2017).
26. A. Ledeboer *et al*., Intrathecal interleukin-10 gene therapy attenuates paclitaxel-induced mechanical allodynia and proinflammatory cytokine expression in dorsal root ganglia in rats. *Brain Behav. Immun.* **21**, 686–698 (2007).
27. Q. Shao, Y. Li, Q. Wang, J. Zhao, IL-10 and IL-1β mediate neuropathic-pain like behavior in the ventrolateral orbital cortex. *Neurochem. Res.* **40**, 733–739 (2015).
28. G. Laumet *et al*., Interleukin-10 resolves pain hypersensitivity induced by cisplatin by reversing sensory neuron hyperexcitability. *Pain* **161**, 2344–2352 (2020).
29. S. Lemmer *et al*., Enhanced spinal neuronal responses as a mechanism for the increased nociceptive sensitivity of interleukin-4 deficient mice. *Exp. Neurol.* **271**, 198–204 (2015).
30. S. Hao, M. Mata, J. C. Glorioso, D. J. Fink, HSV-mediated expression of interleukin-4 in dorsal root ganglion neurons reduces neuropathic pain. *Mol. Pain* **2**, 6 (2006).
31. B. Nie *et al*., AKAP150 involved in paclitaxel-induced neuropathic pain via inhibiting CN/NFAT2 pathway and downregulating IL-4. *Brain Behav. Immun.* **68**, 158–168 (2017).
32. J. Kraus *et al*., Regulation of mu-opioid receptor gene transcription by interleukin-4 and influence of an allelic variation within a STAT6 transcription factor binding site. *J. Biol. Chem.* **276**, 43901–43908 (2001).
33. P. M. Grace, M. R. Hutchinson, S. F. Maier, L. R. Watkins, Pathological pain and the neuroimmune interface. *Nat. Rev. Immunol.* **14**, 217–231 (2014).
34. J. Prado *et al*., Development of recombinant proteins to treat chronic pain. *J. Vis. Exp.*, 57071 (2018).
35. C. Steen-Louws *et al*., Sialic acid-engineered IL4-10 fusion protein is bioactive and rapidly cleared from the circulation. *Pharm. Res.* **37**, 17 (2019).
36. I. Moraga, J. Spangler, J. L. Mendoza, K. C. Garcia, Multifarious determinants of cytokine receptor signaling specificity. *Adv. Immunol.* **121**, 1–39 (2014).
37. R. M. Stroud, J. A. Wells, Mechanistic diversity of cytokine receptor signaling across cell membranes. *Sci. STKE* **2004**, re7 (2004).
38. A. Ullrich, J. Schlessinger, Signal transduction by receptors with tyrosine kinase activity. *Cell* **61**, 203–212 (1990).
39. J. A. Wells, A. M. de Vos, Structure and function of human growth hormone: Implications for the hematopoietins. *Annu. Rev. Biophys. Biomol. Struct.* **22**, 329–351 (1993).
40. X. Wang, P. Lupardus, S. L. Laporte, K. C. Garcia, Structural biology of shared cytokine receptors. *Annu. Rev. Immunol.* **27**, 29–60 (2009).
41. I. Moraga *et al*., Synthekines are surrogate cytokine and growth factor agonists that compel signaling through non-natural receptor dimers. *eLife* **6**, e22882 (2017).
42. H. L. D. M. Willemen *et al*., Identification of FAM173B as a protein methyltransferase promoting chronic pain. *PLoS Biol.* **16**, e2003452 (2018).
43. B. Abrahamsen *et al*., The cell and molecular basis of mechanical, cold, and inflammatory pain. *Science* **321**, 702–705 (2008).
44. P. Honoré, V. Chapman, J. Buritova, J. M. Besson, When is the maximal effect of pre-administered systemic morphine on carrageenin evoked spinal c-Fos expression in the rat? *Brain Res.* **705**, 91–96 (1995).
45. H. Bester, S. P. Hunt, "The expression of c-Fos in the spinal cord: Mapping of nociceptive pathways" in *Immediate Early Genes and Inducible Transcription Factors in Mapping of the Central Nervous System Function and Dysfunction*, L. Kaczmarek, H. A. Robertson, Eds. (Elsevier, 2002), pp. 171–184.
46. C. Abbadie, J. M. Besson, C-fos expression in rat lumbar spinal cord following peripheral stimulation in adjuvant-induced arthritic and normal rats. *Brain Res.* **607**, 195–204 (1993).
47. J. Schadrack, J. M. Castro-Lopes, A. Avelino, W. Zieglgänsberger, T. R. Tölle, Modulated expression of c-Fos in the spinal cord following noxious thermal stimulation of monoarthritic rats. *J. Neurosci. Res.* **53**, 203–213 (1998).
48. T. Hagenacker, J. C. Czeschik, M. Schäfers, D. Büsselberg, Sensitization of voltage activated calcium channel currents for capsaicin in nociceptive neurons by tumor-necrosis-factor-alpha. *Brain Res. Bull.* **81**, 157–163 (2010).
49. C. Steen-Louws *et al*., IL4-10 fusion protein has chondroprotective, anti-inflammatory and potentially analgesic effects in the treatment of osteoarthritis. *Osteoarthritis Cartilage* **26**, 1127–1135 (2018).
50. P. Ray *et al*., Comparative transcriptome profiling of the human and mouse dorsal root ganglia: An RNA-seq-based resource for pain and sensory neuroscience research. *Pain* **159**, 1325–1345 (2018).
51. S. G. Khasar, M. S. Gold, S. Dastmalchi, J. D. Levine, Selective attenuation of mu-opioid receptor-mediated effects in rat sensory neurons by intrathecal administration of antisense oligodeoxynucleotides. *Neurosci. Lett.* **218**, 17–20 (1996).
52. N. Dias, C. A. Stein, Antisense oligonucleotides: Basic concepts and mechanisms. *Mol. Cancer Ther.* **1**, 347–355 (2002).
53. Z. Guan *et al*., Injured sensory neuron-derived CSF1 induces microglial proliferation and DAP12-dependent pain. *Nat. Neurosci.* **19**, 94–101 (2016).
54. K. Inoue, M. Tsuda, S. Koizumi, ATP receptors in pain sensation: Involvement of spinal microglia and P2X(4) receptors. *Purinergic Signal.* **1**, 95–100 (2005).
55. T. Trang, S. Beggs, M. W. Salter, ATP receptors gate microglia signaling in neuropathic pain. *Exp. Neurol.* **234**, 354–361 (2012).
56. M. Calvo *et al*., Following nerve injury neuregulin-1 drives microglial proliferation and neuropathic pain via the MEK/ERK pathway. *Glia* **59**, 554–568 (2011).
57. J. Suthaus *et al*., Forced homo- and heterodimerization of all gp130-type receptor complexes leads to constitutive ligand-independent signaling and cytokine-independent growth. *Mol. Biol. Cell* **21**, 2797–2807 (2010).
58. P. Li, S. Yuan, J. Galipeau, A fusion cytokine coupling GMCSF to IL9 induces heterologous receptor clustering and STAT1 hyperactivation through JAK2 promiscuity. *PLoS One* **8**, e69405 (2013).

59. S. Ng, J. Galipeau, Concise review: Engineering the fusion of cytokines for the modulation of immune cellular responses in cancer and autoimmune disorders. *Stem Cells Transl. Med.* **4**, 66–73 (2015).
60. L. K. Oetjen *et al*., Sensory neurons co-opt classical immune signaling pathways to mediate chronic itch. *Cell* **171**, 217–228.e13 (2017).
61. M. Busch-Dienstfertig, S. González-Rodríguez, IL-4, JAK-STAT signaling, and pain. *JAK-STAT* **2**, e27638 (2013).
62. D. M. White, Contribution of neurotrophin-3 to the neuropeptide Y-induced increase in neurite outgrowth of rat dorsal root ganglion cells. *Neuroscience* **86**, 257–263 (1998).
63. D. M. White, Neurotrophin-3 antisense oligonucleotide attenuates nerve injury-induced Abeta-fibre sprouting. *Brain Res.* **885**, 79–86 (2000).
64. G. Laumet *et al*., T cells as an emerging target for chronic pain therapy. *Front. Mol. Neurosci.* **12**, 216 (2019).
65. G. Laumet *et al*., Resolution of inflammation-induced depression requires T lymphocytes and endogenous brain interleukin-10 signaling. *Neuropsychopharmacology* **43**, 2597–2605 (2018).
66. R. Raoof *et al*., Macrophages transfer mitochondria to sensory neurons to resolve inflammatory pain. bioRxiv:10.1101/2020.02.12.940445 (13 February 2020).
67. M. C. Pils *et al*., Monocytes/macrophages and/or neutrophils are the target of IL-10 in the LPS endotoxemia model. *Eur. J. Immunol.* **40**, 443–448 (2010).
68. M. A. Nassar *et al*., Nociceptor-specific gene deletion reveals a major role for Nav1.7 (PN1) in acute and inflammatory pain. *Proc. Natl. Acad. Sci. U.S.A.* **101**, 12706–12711 (2004).
69. K. Hargreaves, R. Dubner, F. Brown, C. Flores, J. Joris, A new and sensitive method for measuring thermal nociception in cutaneous hyperalgesia. *Pain* **32**, 77–88 (1988).
70. S. R. Chaplan, F. W. Bach, J. W. Pogrel, J. M. Chung, T. L. Yaksh, Quantitative assessment of tactile allodynia in the rat paw. *J. Neurosci. Methods* **53**, 55–63 (1994).
71. N. Eijkelkamp *et al*., GRK2: A novel cell-specific regulator of severity and duration of inflammatory pain. *J. Neurosci.* **30**, 2138–2149 (2010).
72. M. J. Ripple *et al*., Immunomodulation with IL-4R alpha antisense oligonucleotide prevents respiratory syncytial virus-mediated pulmonary disease. *J. Immunol.* **185**, 4804–4811 (2010).
73. L. S. Stone, L. Vulchanova, The pain of antisense: In vivo application of antisense oligonucleotides for functional genomics in pain and analgesia. *Adv. Drug Deliv. Rev.* **55**, 1081–1112 (2003).
74. N. Eijkelkamp *et al*., A role for Piezo2 in EPAC1-dependent mechanical allodynia. *Nat. Commun.* **4**, 1682 (2013).
75. M. Meijer *et al*., Inhibition of voltage-gated calcium channels after subchronic and repeated exposure of PC12 cells to different classes of insecticides. *Toxicol. Sci.* **147**, 607–617 (2015).
76. O. Söderberg *et al*., Characterizing proteins and their interactions in cells and tissues using the in situ proximity ligation assay. *Methods* **45**, 227–232 (2008).
77. M. M. Bradford, A rapid and sensitive method for the quantitation of microgram quantities of protein utilizing the principle of protein-dye binding. *Anal. Biochem.* **72**, 248–254 (1976).
78. S. Andrews, FastQC: A quality control tool for high throughput sequence data. www.bioinformatics.babraham.ac.uk/projects/fastqc. Accessed 26 February 2021.
79. A. Dobin *et al*., STAR: Ultrafast universal RNA-seq aligner. *Bioinformatics* **29**, 15–21 (2013).
80. F. Cunningham *et al*., Ensembl 2015. *Nucleic Acids Res.* **43**, D662–D669 (2015).
81. J. Prado *et al*., Next generation sequencing reveals different transcriptome induced by IL4-10 fusion protein (IL4-10 FP) compared to the combination of cytokines in mice with inflammatory pain. Gene Expression Omnibus. https://www.ncbi.nlm.nih.gov/geo/query/acc.cgi?acc=GSE150795. Deposited 18 May 2020.